

RESEARCH

Open Access



X-linked ubiquitin-specific peptidase 11 (USP11) increases susceptibility to Cushing's disease in women

Tao Zhang^{1,2†}, Yanting Liu^{2†}, Fang Liu^{2†}, Kaiyu Guo^{1,2}, Runhua Tang¹, Jingwei Ye^{1,2}, Li Xue^{2,3,4}, Zhipeng Su^{1*} and Zhe Bao Wu^{1,2,3*}

Abstract

The incidence of pituitary adrenocorticotrophic hormone (ACTH)-secreting PitNETs, commonly known as ACTH PitNETs, is significantly higher in females; however, the underlying causes for this gender disparity remain unclear. In this study, we analyzed the expression of deubiquitinating enzymes in functioning ACTH PitNETs from both male and female subjects using RNA sequencing and identified USP11 as a potential susceptibility factor contributing to the higher prevalence of these PitNETs in females. Further investigation revealed that USP11 expression is markedly elevated in female functioning ACTH PitNETs, with levels significantly higher than those observed in male PitNETs and normal pituitary tissue. Experimental data indicate that USP11 promotes the transcription of proopiomelanocortin (POMC) and the secretion of ACTH. In contrast, knockdown of USP11 leads to a substantial reduction in both POMC transcription and ACTH secretion, as demonstrated in both in vitro and in vivo models. Mechanistically, we found that USP11 facilitates the deubiquitination of the key transcription factor TPIT in functioning ACTH PitNETs, enhancing its protein stability and thereby promoting POMC transcription and ACTH secretion. Additionally, virtual screening identified Lomitapide and Nicergoline as potential inhibitors of USP11, reducing POMC expression and ACTH secretion. Thus, USP11 emerges as a potential therapeutic target, and drugs aimed at inhibiting its function could benefit women with Cushing's disease.

Keywords Cushing's disease, Sex differences, USP11, TPIT, Adrenocorticotrophic hormone

[†]Tao Zhang, Yanting Liu and Fang Liu contributed equally to this work.

*Correspondence:

Zhipeng Su
drsuzhipeng@163.com
Zhe Bao Wu
zhebaowu@aliyun.com

¹Department of Neurosurgery, First Affiliated Hospital of Wenzhou Medical University, Wenzhou 325000, China

²Department of Neurosurgery, Center of Pituitary Tumor, Ruijin Hospital, Shanghai Jiao Tong University School of Medicine, Shanghai 200025, China

³Department of Neurosurgery, Center for Immune-Related Diseases, Shanghai Institute of Immunology, Ruijin Hospital, Shanghai Jiao Tong University School of Medicine, Shanghai 200025, China

⁴Shanghai Center for Brain Science and Brain-Inspired Technology, Shanghai 200022, China



Introduction

Adrenocorticotrophic hormone (ACTH)-secreting PitNETs, commonly known as Cushing's disease, are distinguished by the expression of the upstream transcription factor TPIT, which regulates the pro-opiomelanocortin (POMC) gene—the precursor for ACTH transcription and secretion [1]. These PitNETs show positive immunohistochemical staining for ACTH. Patients with ACTH-secreting PitNETs suffer from hypercortisolism due to excess ACTH, leading to a spectrum of serious endocrine and metabolic disorders, such as hypertension, diabetes mellitus, hyperlipidemia, osteoporosis, central obesity, and cardiovascular diseases [2]. These complications affect multiple organs and systems, presenting a substantial clinical risk, with mortality rates that are four times higher than in the general population [2, 3].

ACTH PitNETs exhibit a strong gender predilection, primarily affecting young women aged 35 to 44 years, with an incidence rate 5 to 10 times higher in women than in men [4]. An analysis of 2,230 patients with pituitary neuroendocrine tumors (PitNETs) found that female patients with ACTH PitNETs outnumbered male patients by more than fourfold [5]. At the Endocrinology Clinical Center at Sofia Medical University in Bulgaria, of the 386 cases of Cushing's disease managed, 84% were female [6]. Similarly, data from the Pituitary Adenoma Treatment Center at Santa Clara Hospital showed that 92.3% of patients who underwent surgery for ACTH PitNETs were women [7]. Analysis from Huashan Hospital, affiliated with Fudan University, indicates that among 124 patients who had ACTH PitNETs surgically excised, only 17.2% were male [8]. Our recent research further supports these findings, revealing that women constitute 90% of the ACTH adenoma patient population [9]. Despite these statistics, the underlying reasons for the female predisposition to ACTH PitNETs remain unknown.

Deubiquitination processes are crucial in the pathogenesis and progression of ACTH PitNETs [10, 11]. Disruption of the dynamic balance between ubiquitination and deubiquitination not only promotes tumor initiation and progression but may also influence gender differences in tumor pathogenesis [12, 13]. In males, androgens modulate the expression of USP18 via binding and activation of the androgen receptor (AR) transcription factor, thereby promoting tumor initiation and progression [14]. Conversely, the X chromosome-linked genes USP9X and USP11—both of which escape X chromosome inactivation—are expressed at higher levels in females, contributing to the pathogenesis of female breast cancer [15, 16]. However, the specific roles and mechanisms by which the ubiquitin-proteasome system contributes to gender differences in the pathogenesis of ACTH PitNETs remain unexamined.

In this study, we found that USP11 promotes the deubiquitination of TPIT, enhancing POMC transcription and ACTH secretion, thereby increasing susceptibility to Cushing's disease in women. Additionally, virtual screening identified potential USP11 inhibitors, suggesting a therapeutic strategy for Cushing's disease in female patients.

Materials and methods

Clinical data and human tissues samples

Samples of pituitary adenomas (PAs) were obtained from patients undergoing surgical procedures at Ruijin Hospital during the period spanning from 2016 to 2023. The study received ethical approval from the Ethical Review Board of Ruijin Hospital, affiliated with Shanghai Jiao Tong University School of Medicine. All patients whose tumor tissues were utilized in this study provided written, informed consent. The information of patients was listed in Supplementary Table 1.

Cell culture and reagents

The cell lines were tested for mycoplasma contamination prior to use using the Mycoplasma Stain Assay kit (Beyotime, C0296). HEK293T and AtT-20 cells were kindly provided by Cell Bank, Chinese Academy of Sciences. In cell culture, the AtT-20 cells were cultivated in Ham's/F2 K (Kaighn's) medium (Basal Media, L450KJ, Shanghai, China) supplemented with 2.5% (v/v) fetal bovine serum (FBS, Basal Media, S660JJ, Shanghai, China) and 15% horse serum (Absin, abs989, Shanghai, China). The HEK293T cells were cultured in Dulbecco's Modified Eagle Medium (DMEM, Basal Media, L110KJ, Shanghai, China) supplemented with 10% FBS. The cell lines were maintained in a humidified atmosphere at 37 °C with 5% CO₂.

Plasmids

See Supplementary Table 2 for details. pLVshRNA-EGFP(2 A)Puro cloning vector was used to generate the shRNAs targeting gene at various regions. Mouse USP11 knockdown adenoviruses were purchased from Vigene Biosciences. The sequences of the shRNAs can be found in Supplementary Table 3.

Stable cell lines

HEK293T cells were transfected with plasmids, including targeting plasmid, pMD2.G and pSPAX2. After 48 hours' post-transfection, media containing the virus were collected and filtered through 0.45 μm nitrocellulose filters (Millipore, SLHV033RS). The virus was then concentrated using PEG8000 (5 × PEG8000: 150 mm NaCl; 25% PEG8000) and used to infect AtT-20 cells. The stable cells were selected using puromycin at 1 μg/ml (Beyotime, ST551).

Immunoblot analysis

Total proteins were extracted using Triton X-100 lysis buffer supplemented with protease inhibitors (NCM Biotech, P003) and sonicated with a Qsonica Q700 Sonicator. Protein concentration was determined using a BCA protein assay kit (Yoche Biotech, YSD-500T) and measured at 562 nm with a Biotek 800 TS microplate reader. Equal amounts of whole-cell lysates were prepared with SDS-PAGE loading buffer and subjected to SDS-PAGE analysis, followed by transfer to polyvinylidene difluoride membranes (Millipore, ISEQ10100). The specified antibodies were listed in Supplementary Table 4.

Immunohistochemistry (IHC)

The immunohistochemistry experiment was conducted as previously described [17]. The expression levels of USP11 were assessed using the H-Score method [$H\text{-SCORE} = \sum(\text{PI} \times I) = (\text{percentage of cells with weak intensity} \times 1) + (\text{percentage of cells with moderate intensity} \times 2) + (\text{percentage of cells with strong intensity} \times 3)$], employing QuantCenter 2.3 software. The quantification of expression in each sample was conducted in 10 randomly selected fields (at a magnification of 400 \times) for each case, by two impartial observers who were unaware of the participants' medical characteristics.

Quantitative real-time PCR (qRT-PCR)

Total RNA was extracted from cells using a total RNA extraction kit (NCM Biotech, M5105). RNA concentration was measured with a DS-11 microphotometer. cDNA synthesis was performed using a cDNA synthesis kit (ABclonal, RK20429). Quantitative real-time polymerase chain reaction (qRT-PCR) was conducted with the SYBR Green qPCR kit (ABclonal, RK21203) following the manufacturer's instructions, using an ABI 7500 Real-Time PCR System (Applied Biosystems). The primer sequences for qRT-PCR are listed in Supplementary Table 5.

Xenograft model

The Ethical Review Board at Shanghai Jiao Tong University School of Medicine's Ruijin Hospital approved of the study's animal experimentation. The protocols followed the Institutional Animal Care and Use Committee's (IACUC) guidelines. Four-week-old nu/nu female mice were procured and maintained in a controlled specific pathogen-free environment. One million AtT-20 cells were mixed with Matrigel (Yeasten, 40187) and subcutaneously injected.

ELISA

1 mL of culture medium containing 40,000 cells was added to each well of a 12-well plate. After 24 h, the supernatant was collected and centrifuged at 4 °C at

2,000 g for 20 min. ACTH levels were measured using an ELISA kit (Abcam, ab263880).

Isolation and cultivation of pituitary tumor cells

To culture primary pituitary tumor cells, freshly collected PA tissues were washed with HBSS, cut into ~3 mm pieces, and digested with HBSS (Gibco, 14025092) containing 100 U/mL collagenase type IV (Gibco, 17104019) at 37 °C for 6–8 h. After digestion, cells were filtered through a 100 μm strainer, washed with HBSS, and treated with ACK Lysing Buffer for 5 min. They were then cultured in DMEM with 10% FBS in a 10 cm dish. After 48 h of incubation, the suspended tumor cells were used for experiments. The relevant patient data can be found in Supplementary Table 6.

Mass spectrometry (MS)

The primary corticotroph tumor cells were infected with Flag-USP11 adenovirus at a multiplicity of infection (MOI) of 10. Cells were lysed using a Triton X-100 lysis buffer composed of 150 mM NaCl, 50 mM Tris, and 1% Triton X-100 (pH 7.5). The immunoprecipitation complex was isolated using anti-DYKDDDDK affinity beads obtained from Smart-lifesciences Biotechnology. The beads were washed five times with Triton X-100 lysis buffer and then eluted with elution buffer containing 8 M urea and 100 mM Tris (pH 8.0). The eluted proteins were subsequently analyzed using MS.

Co-immunoprecipitation (Co-IP)

The cells were lysed using Triton X-100 lysis buffer supplemented with a protease inhibitor cocktail and sonicated. The resulting whole-cell lysates were then incubated overnight with 1–2 μg of antibody, followed by a 1-hour incubation with rProtein A/G Beads (Smart-lifesciences Biotechnology, SA032025) at room temperature. The immunoprecipitates were washed five times with lysis buffer and subsequently analyzed by immunoblotting.

GST pulldown assay

GST and GST-TPIT were expressed in BL21 competent cells and purified using glutathione-agarose beads (GE Healthcare, 17075601) according to the manufacturer's instructions. USP11-His proteins were purified using Ni-NTA agarose beads (Qiagen, 18735328) following the manufacturer's protocols. The purified USP11-His and GST-TPIT proteins were incubated in pulldown buffer [50 mM Tris-Cl (pH 8.0), 200 mM NaCl, 1 mM EDTA, 1% NP-40, 1 mM DTT, and 10 mM MgCl₂] for 2 h at 4 °C. The beads were then washed five times with pulldown buffer and analyzed by immunoblotting.

Immunofluorescence microscopy

AtT-20 cells were infected with lentivirus carrying Flag-TPIT and subsequently seeded in a 12-well plate pre-coated with matrigel (Absin, abs9410). The cells were fixed in a 4% formaldehyde solution for 20 minutes, followed by washing with PBS. Next, the cells were permeabilized with cold 0.2% Triton X-100 for 15 minutes and then incubated overnight at 4°C with USP11 and Flag antibodies after blocking with 3% BSA. Afterward, secondary antibodies conjugated with Alexa 488 (CST, 4412S) or Alexa 555 (CST, 4409S) were applied for 1 hour at 37°C. Nuclei were stained with DAPI (Beyotime, C1002), and the stained slices were observed using a Zeiss LSM880 lightning confocal microscope (Carl Zeiss AG, Oberkochen, Germany).

Ubiquitination assay

HEK293T cells were co-transfected with plasmids for 24 h. Following transfection, the cells were lysed with RIPA lysis buffer (50 mM Tris-Cl, 150 mM NaCl, 5 mM EDTA, 1% Triton X-100, 0.5% sodium pyrophosphate, 0.1% SDS, pH 7.4) supplemented with a protease inhibitor cocktail. The whole-cell lysates were then incubated overnight with anti-DYKDDDDK affinity beads. Afterward, the beads were washed five times with lysis buffer and analyzed via immunoblotting using the appropriate antibodies.

Cycloheximide (CHX) chase assay

The cells were treated with 100 µg/ml CHX (ApexBio, A8244) and collected at specified time intervals for subsequent immunoblotting analysis.

Virtual screening analysis

In the PubChem database (<https://pubchem.ncbi.nlm.nih.gov/>), the standard SMILES format content of target active molecules was searched. RDKit (2023.09.1) was used for the structural standardization and processing of compounds, generating a molecular library suitable for virtual screening. All molecules were converted into the required three-dimensional structures (SDF format) using OpenBabel 2.4.1. The structure of the protein USP11 was predicted using AlphaFold software. The binding pocket of the protein USP11 was predicted using an internally developed software—PLI (Protein Ligand Interaction)—to determine the central position and size of the binding region for active molecules on the protein. The central coordinates were (4.8, 4.1, 11.6) Å, and the dimensions of the binding box were 26 Å, 22 Å, and 26 Å. Docking was performed using AutoDockTools 1.5.6 and Vina 1.1.2. The energy difference range at the binding site was set to 4 kcal/mol, and the exhaustiveness parameter was set to 12. The best binding modes of the ligands were searched using a combination of Genetic

Algorithm (GA) and Particle Swarm Optimization (PSO). A scoring function based on empirical formulas was used to evaluate the binding results of all compounds with the target protein, obtaining the binding energy (affinity) and binding modes for each compound. Potential compounds with lower binding energies were selected, and the results were visualized using PyMOL 2.2.0. PLIP (Protein-Ligand Interaction Profiler) was used to analyze the binding modes and interactions of potential active compounds with the protein USP11. The relevant data can be found in Supplementary Table 7.

Statistical analysis

Data analysis was performed using GraphPad Prism version 7 (GraphPad Software, La Jolla, CA, USA) and presented as means ± standard error of the mean (SEM). Statistical analyses included two-tailed t-tests, one-way ANOVA and two-way ANOVA. Statistical significance was denoted by $p < 0.05$ and visually represented in Figs. by one asterisk ($p < 0.05$), two asterisks ($p < 0.01$), or three asterisks ($p < 0.001$).

Results

RNA sequencing identified USP11 as a potential susceptibility factor for functioning ACTH PitNETs in women

Mutations in the deubiquitinating enzymes USP8 and USP48 have been shown to promote the development of ACTH PitNETs, suggesting that these enzymes play a crucial role in the pathogenesis of the disease [10, 11]. To further investigate the role of deubiquitinating enzymes in the observed gender-specific differences in functioning ACTH PitNETs, we conducted a gender-based differential analysis of 105 deubiquitinating enzymes using RNA sequencing. The analysis included data from 13 female and 5 male patients with functioning ACTH PitNETs, revealing that 15 deubiquitinating enzymes were upregulated in females, with no enzymes showing downregulated. Additionally, we analyzed datasets from the European Bioinformatics Institute (EMBL-EBI) ArrayExpress (accession number E-MTAB-7768), which included 21 female and 5 male samples. In this dataset, 19 deubiquitinating enzymes were upregulated in females, with no downregulation observed. In both datasets, the expression levels of USP11, USP22, USP46, OTUD3, and JOSD1 were significantly elevated in female PitNETs (Fig. 1A-C, Supplementary Fig. 1A-D). No significant differences were observed between males and females in the expression of USP8 and USP48 (Supplementary Fig. 1E-F). To further explore the role of these five candidate genes in the pathogenesis of functioning ACTH PitNETs, we overexpressed them in the AtT-20 cell line. Our results showed that the overexpression of USP11 specifically led to an increase in POMC expression, while

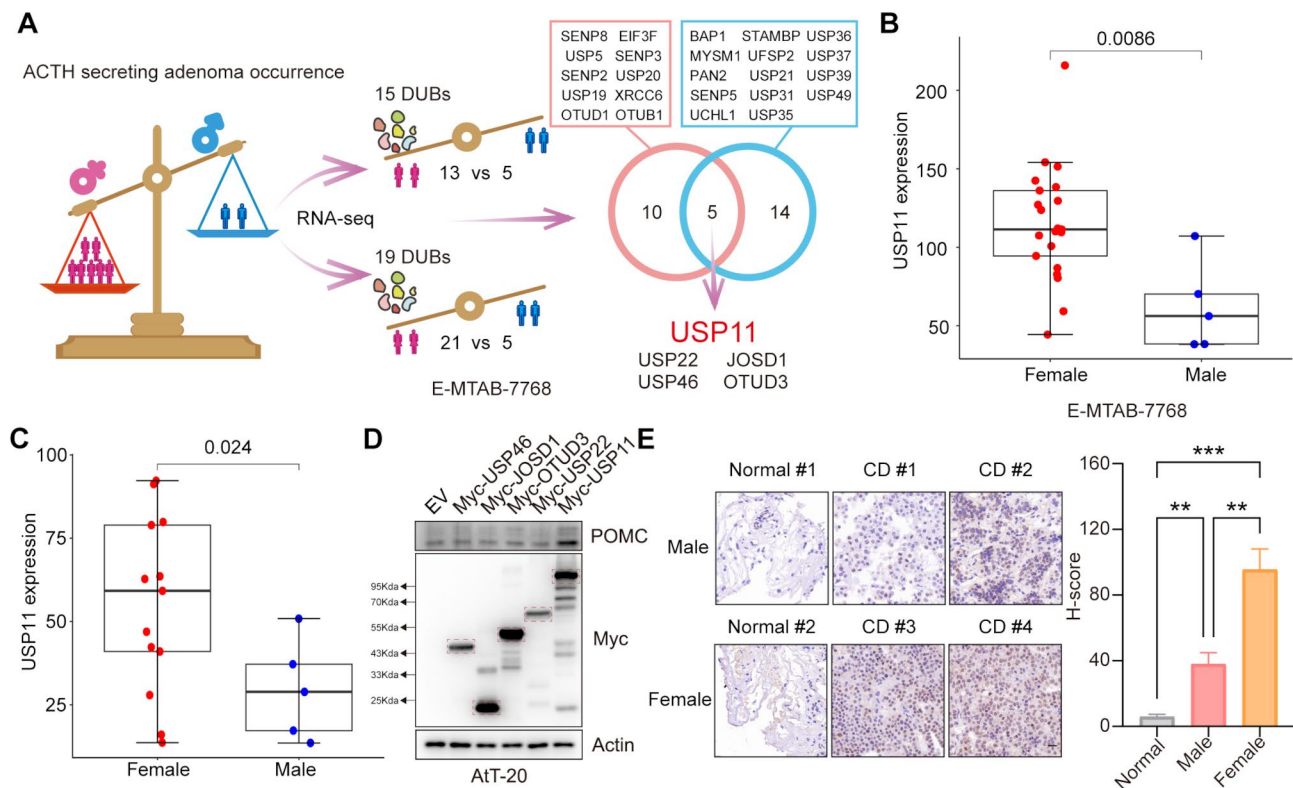


Fig. 1 RNA sequencing identified USP11 as a susceptibility factor for women with functioning ACTH PitNETs. **(A)** Differential expression of deubiquitinating enzymes in male and female Cushing's disease based on our data and the dataset from EMBL-EBI Array Express (accession numbers E-MTAB-7768). **(B)** The expression of USP11 in female and male PitNETs (accession numbers E-MTAB-7768). Female Cushing's disease = 21, male Cushing's disease = 5. Data are presented as mean \pm SEM values. **(C)** The expression of USP11 in female and male PitNETs. Female Cushing's disease = 13, male Cushing's disease = 5. Data are presented as mean \pm SEM values. **(D)** The AtT-20 cells were infected with indicated genes and then immunoblotted. **(E)** The representative IHC images of USP11 in normal pituitary, male and female functioning ACTH PitNETs with analysis. Scale bar, 50 μ m. Normal pituitary = 5, female Cushing's disease = 13, male Cushing's disease = 5. Data are presented as mean \pm SEM values. ** p < 0.01, *** p < 0.001

the other genes did not produce similar effects (Fig. 1D). As a result, USP11 was selected as the focus for further analysis. Immunohistochemical analysis confirmed that USP11 expression is significantly elevated in functioning ACTH PitNETs in females, with markedly higher levels compared to male PitNETs and normal pituitary tissue (Fig. 1E).

Therefore, USP11 may serve as a potential susceptibility factor contributing to the higher incidence of functioning ACTH PitNETs observed in females.

USP11 promotes POMC transcription and ACTH secretion

To investigate the role of USP11 in ACTH-secreting PitNETs, we overexpressed USP11 in AtT-20 cells. The overexpression of USP11 resulted in increased POMC protein levels in these cells (Fig. 1E). Additionally, qPCR analysis indicated that USP11 enhanced the *Pomc* transcription without affecting the transcription of *Tpit* in AtT-20 cells (Fig. 2A, Supplementary Fig. 2A). Similarly, knockdown of USP11 led to a reduction in POMC protein expression (Fig. 2B), and suppressed *Pomc* transcription without affecting *Tpit* transcription (Fig. 2C, Supplementary

Fig. 2B). Importantly, we evaluated the effect of USP11 on ACTH secretion using enzyme-linked immunosorbent assay (ELISA), which demonstrated that overexpression of USP11 increased ACTH secretion, whereas knockdown reduced ACTH secretion in AtT-20 cells (Fig. 2D-E). To explore the impact of USP11 on POMC and ACTH in vivo, we implanted USP11 knockdown or control AtT-20 cells into nude mice. Immunohistochemistry analysis revealed that USP11 knockdown resulted in decreased POMC levels (Fig. 2F). Notably, USP11 knockdown significantly inhibited ACTH secretion in vivo (Fig. 2G).

These findings collectively indicate that USP11 enhances the transcription of POMC and promotes ACTH secretion.

USP11 directly interacts with the transcription factor TPIT

EGFR and the ERK/MAPK signaling pathway are known to promote the development of ACTH PitNETs [10, 11]. USP11 deubiquitinates EGFR, stabilizing its protein levels and activating the ERK/MAPK pathway [18, 19]. However, overexpression of USP11 did not significantly affect EGFR or ERK signaling in AtT-20 cells (Supplementary

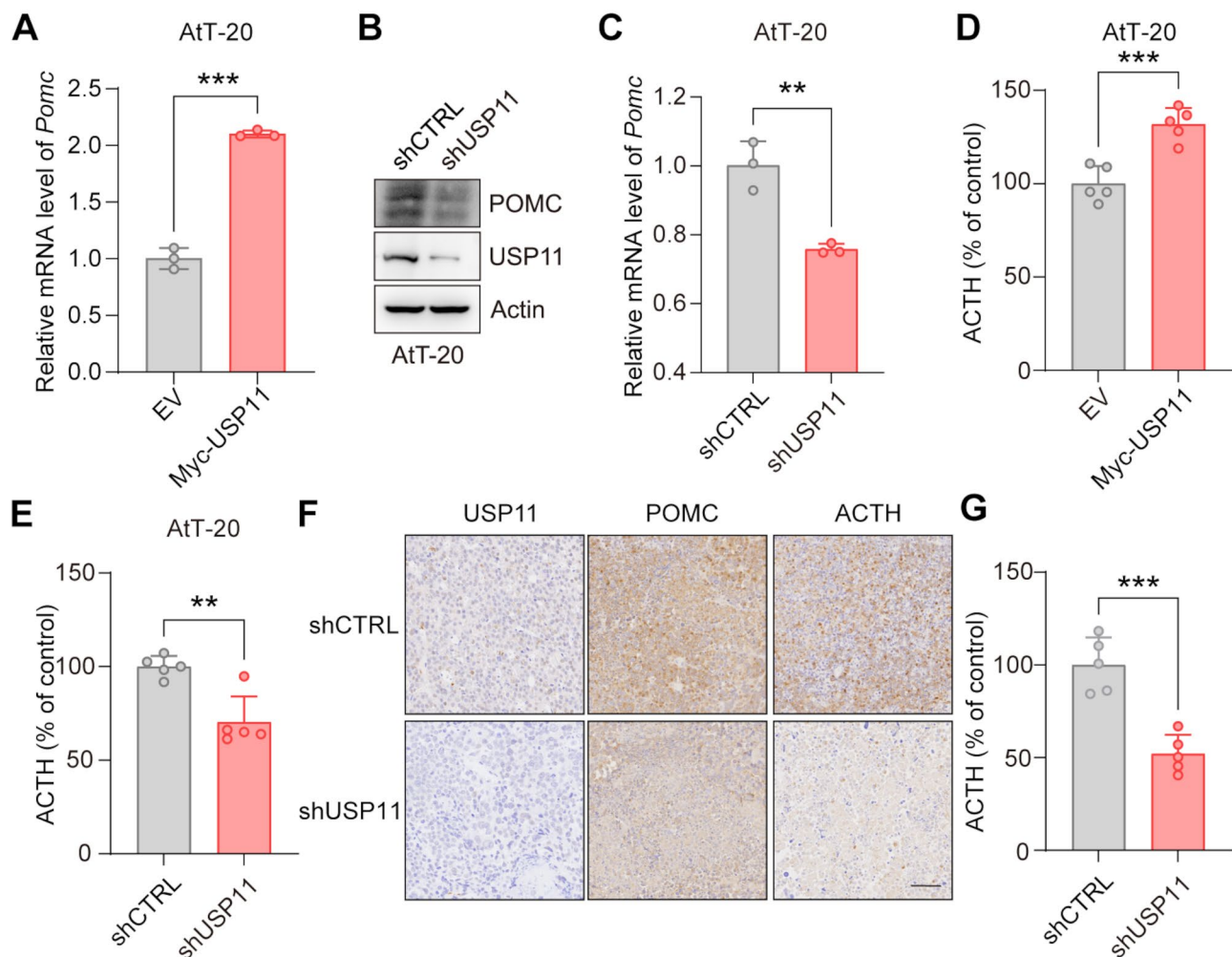


Fig. 2 USP11 regulates POMC expression and ACTH secretion. **(A)** qPCR showed that USP11 promoted the transcription of *Pomc* in AtT-20 cells. Data are presented as mean \pm SEM values. $n=3$. *** $p < 0.001$. **(B-C)** Knockdown of USP11 suppressed the protein **(C)** and mRNA **(D)** expression of POMC in AtT-20 cells. Data are presented as mean \pm SEM values. ** $p < 0.01$. **(D-E)** USP11 regulated the secretion of ACTH in AtT-20 cells. The secretion of ACTH from stable AtT-20 cells with USP11 overexpression **(D)** or knockdown **(E)** was measured by ELISA. Data are presented as mean \pm SEM values. $n=5$. ** $p < 0.01$, *** $p < 0.001$. **(F)** Immunohistochemistry of xenograft tumors. Representative IHC images of USP11, POMC and ACTH in xenograft tumors with USP11 knockdown compared to control. Scale bar, 50 μ m. **(G)** Knockdown of USP11 inhibited ACTH secretion in vivo, which was measured by ELISA in nude mice with xenograft tumors. Data are presented as mean \pm SEM values. $n=5$. *** $p < 0.001$

Fig. 3A). Estradiol is known to stimulate USP11 expression in breast cancer [15], but Estradiol and progesterone failed to upregulate USP11 levels in AtT20 and pituitary primary cells (Supplementary Fig. 3B-C). To clarify the molecular mechanism by which USP11 regulates POMC transcription and ACTH secretion, we performed coimmunoprecipitation (Co-IP) and mass spectrometry (MS) experiments to identify potential proteins associated with USP11 in corticotropin cells. Among the interacting proteins, TPIT was selected as a promising candidate for further investigation (Fig. 3A). The interaction between USP11 and TPIT was further validated by Co-IP in HEK-293T cells, where USP11 was shown to interact with TPIT. Endogenous USP11 was also observed to bind with TPIT in AtT-20 cells (Fig. 3B-C). In vitro,

purified His-USP11 directly interacted with a glutathione S-transferase (GST)-TPIT fusion protein, but not with GST alone (Fig. 3D). Moreover, immunofluorescence analysis revealed that TPIT and USP11 co-localized in AtT-20 cells (Fig. 3E).

Thus, these results suggest that USP11 interacts directly with the transcription factor TPIT.

USP11 deubiquitinates TPIT

To further characterize the mechanism by which USP11 regulates TPIT, we identified USP11 as a deubiquitinase that deubiquitinates TPIT. Knockdown of USP11 led to increased TPIT ubiquitination (Fig. 4A-B). To investigate the interaction region between USP11 and TPIT, Co-IP experiments revealed that USP11 lacking the USP

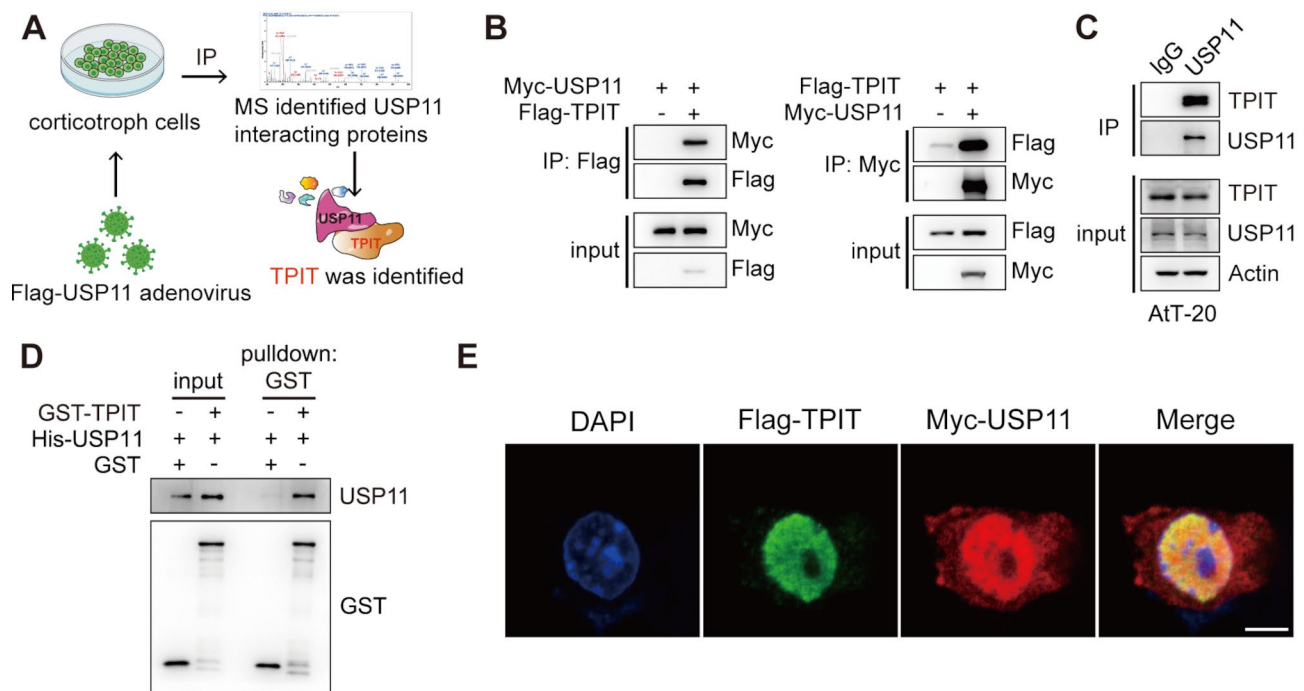


Fig. 3 USP11 interacts with the transcription factor TPIT. **(A)** Flowchart for identifying potential proteins that interact with USP11. USP11 and its interacting proteins were immunoprecipitated and identified using mass spectrometry. **(B-C)** Interaction of TPIT with USP11. External **(B)** and endogenous **(C)** Co-IP experiments were performed to detect the interaction between TPIT and USP11. **(D)** The direct interaction between USP11 and TPIT was determined by GST pull-down assay. **(E)** Co-localization of Flag-TPIT and USP11 in AtT20 cells. Scale bar, 5 μm

domain failed to interact with TPIT (Fig. 4C-D). Ubiquitination assays showed that USP11, when missing the USP domain but retaining the DUSP domain, was unable to deubiquitinate TPIT (Fig. 4E). To identify the lysine (K) residues on TPIT that are deubiquitinated by USP11, we constructed several TPIT mutants (3KR, 4KR, 5KR, and 12KR), as previously described [9]. Ubiquitination assays indicated that TPIT mutants 4KR, 5KR, and 12KR exhibited decreased ubiquitination by USP11 (Fig. 4F). Additionally, our previous research indicated that the ubiquitin ligase TRIM65 enhances TPIT ubiquitination, while overexpression of USP11 reduced TPIT ubiquitination by TRIM65 (Fig. 4G).

Overall, our findings indicate that USP11 interacts with and reduces the ubiquitination of TPIT via its USP domain.

USP11 stabilizes TPIT by reducing its proteasomal degradation

To investigate the regulatory effect of USP11 on TPIT expression, USP11 was overexpressed in HEK-293T and AtT-20 cells. The results showed that USP11 overexpression increased TPIT protein levels in both cell lines (Fig. 5A). Furthermore, USP11 overexpression mitigated the reduction in TPIT levels induced by TRIM65 in HEK-293T cells (Fig. 5B). Cycloheximide (CHX) chase assays further revealed that USP11 overexpression prolonged

the half-life of TPIT protein in both HEK-293T and AtT-20 cells (Fig. 5C-D). Additionally, knockdown of USP11 decreased the half-life of TPIT in these cells (Fig. 5E-F). Additionally, USP11 knockdown led to a reduction in TPIT protein levels, which could be reversed by inhibiting proteasomal activity with the inhibitor MG132, suggesting that USP11 regulates TPIT levels through the proteasomal pathway (Fig. 5G). Immunohistochemistry analysis also showed reduced TPIT levels in vivo following USP11 knockdown (Fig. 5H).

Collectively, these findings demonstrate that USP11 stabilizes TPIT by suppressing its proteasomal degradation.

Lomitapide and Nicergoline inhibit USP11 function, reducing POMC expression and ACTH secretion

At present, there are no specific USP11 inhibitors. In this study, we aimed to explore potential USP11 inhibitors and investigate whether inhibiting USP11 could serve as a therapeutic strategy for functioning ACTH PitNETs in females. Virtual screening is an effective approach for identifying inhibitors, as demonstrated in previous research [20]. We performed structure-based virtual screening to identify USP11 inhibitors targeting the USP domain. Binding affinity is a critical factor in evaluating effective USP11 inhibitors. Starting with a virtual library of 10,637 compounds, we selected 12 potential inhibitors

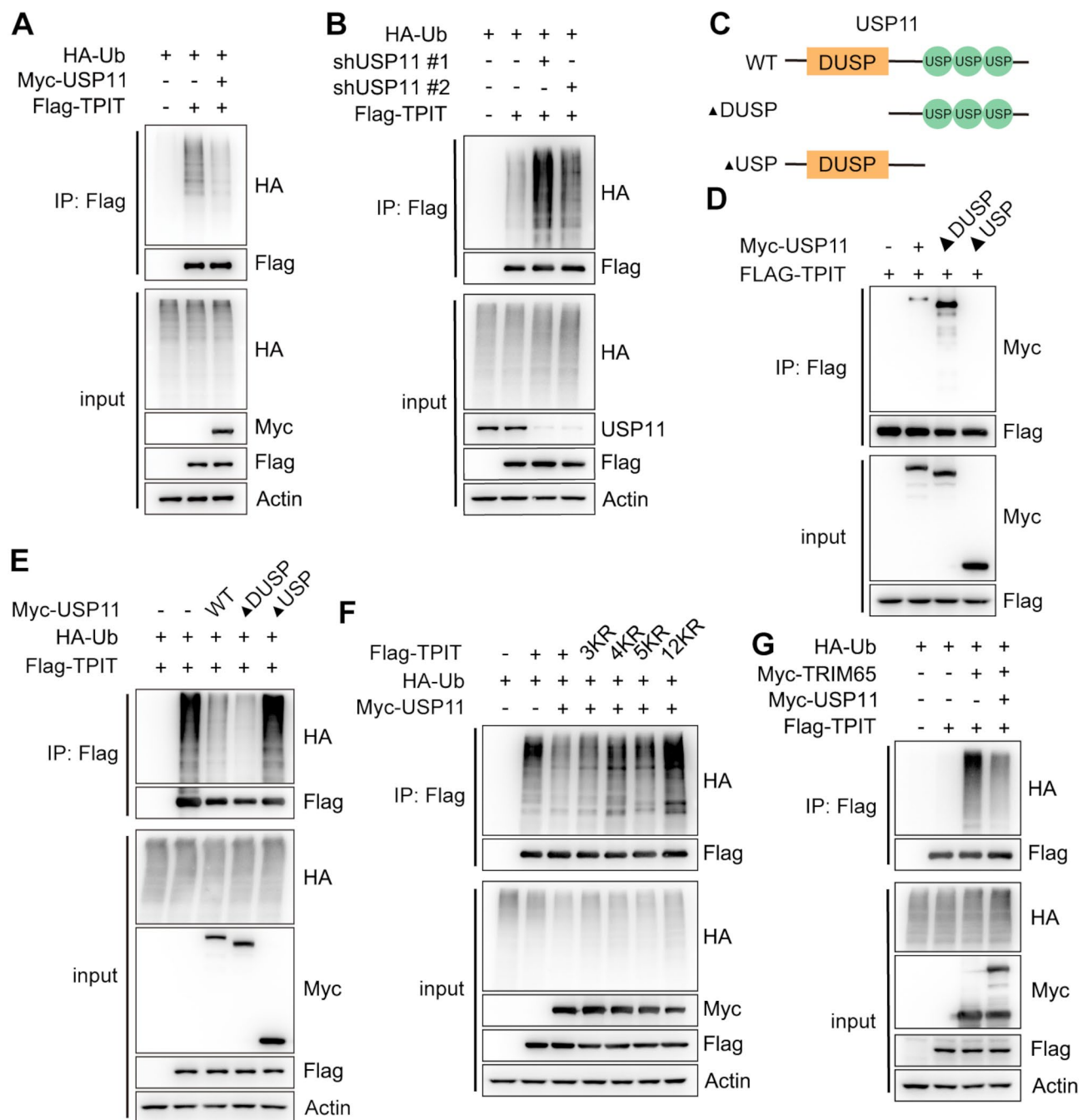


Fig. 4 USP11 decreases the ubiquitination of TPIT. **(A)** USP11 suppressed the ubiquitination of TPIT. HEK293T cells were transfected with the indicated plasmids, and cell lysates were analyzed by ubiquitination assays. **(B)** Knockdown of *USP11* increased TPIT ubiquitination. **(C)** Schematic showing wild-type USP11 and its truncated forms. **(D)** USP11 lacking the USP domain was unable to interact with TPIT. The interaction between Flag-TPIT and Myc-tagged USP11 or its truncated mutants was detected by Co-IP. **(E)** Ubiquitination assays showed that USP11 lacking the USP domains failed to deubiquitinate TPIT. **(F)** Ubiquitination assays showed reduced deubiquitination of TPIT with the 4KR, 5KR, and 12KR mutations by USP11. **(G)** Ubiquitination assays demonstrated that overexpression of USP11 resulted in a decrease in TPIT ubiquitination by TRIM65

for further validation based on binding affinity and their potential as treatments for functioning ACTH PitNETs (Fig. 6A). Further investigations revealed that Bemcentinib, AC628, Lomitapide, and Nicergoline reduced TPIT and POMC protein levels without affecting USP11

protein levels (Fig. 6B). Ubiquitination assays indicated that Lomitapide and Nicergoline suppressed deubiquitination activity of USP11, whereas Bemcentinib and AC628 failed (Fig. 6C). Additionally, Lomitapide and Nicergoline affected TPIT ubiquitination when USP11

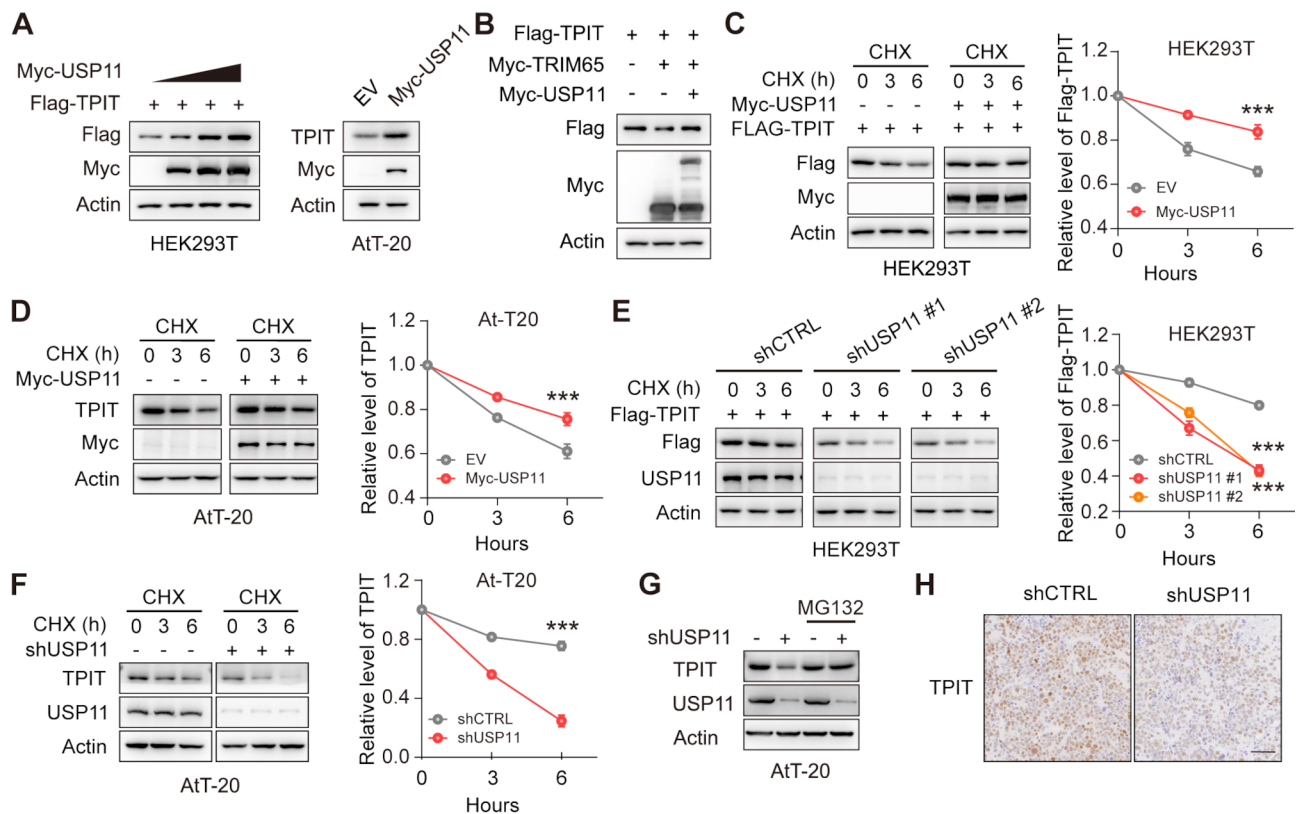


Fig. 5 USP11 mediates the proteasomal degradation of TPIT. **(A)** Overexpression of USP11 increased TPIT protein levels in Flag-TPIT stable HEK-293T and AtT-20 cells. **(B)** USP11 overexpression mitigated the reduction of TPIT levels induced by TRIM65 in Flag-TPIT stable HEK293T cells. **(C-D)** CHX chase assays showed that overexpression of USP11 extend the half-life of TPIT in Flag-TPIT stable HEK-293T **(C)** and AtT-20 **(D)** cells. The cells were treated with CHX (100 μ M) for 0, 3, or 6 h. The relative ratio of TPIT/actin was determined by ImageJ. Data are presented as mean \pm SEM values. n.s., not significant; $n=3$. $***p<0.001$. **(E-F)** CHX chase assays showed that knockdown of USP11 decrease the half-life of TPIT in Flag-TPIT stable HEK-293T **(E)** and AtT-20 **(F)** cells. The cells were treated with CHX (100 μ M) for 0, 3, or 6 h. The relative ratio of TPIT/actin was determined by ImageJ. Data are presented as mean \pm SEM values. n.s., not significant; $n=3$. $***p<0.001$. **(G)** Proteasome inhibitor MG132 (20 μ M) reversed the decrease in TPIT protein levels caused by the knockdown of USP11 in AtT-20 cells. **(H)** Immunohistochemistry of xenograft tumors. Representative IHC images of TPIT in xenograft tumors with USP11 knockdown compared to control. Scale bar, 50 μ m

was knocked down (Fig. 6D). Both compounds also suppressed *Pomc* transcription but had no effect on *Tpit* transcription in AtT-20 cells (Fig. 6E, Supplementary Fig. 6A). Notably, as the concentration of Lomitapide and Nicergoline increased from 0 to 1 μ M, POMC and TPIT protein levels decreased (Fig. 6F). Lomitapide and Nicergoline reduced TPIT protein levels, and knockdown of USP11 reversed this effect, suggesting that Lomitapide and Nicergoline regulate TPIT by inhibiting USP11 activity (Fig. 6G). Additionally, these compounds lowered TPIT and POMC protein levels, and this reduction was reversed by inhibiting proteasomal activity with MG132, suggesting that the downregulation of TPIT occurs via the proteasomal pathway (Fig. 6H). Subsequent ELISA analysis of ACTH secretion showed that both compounds significantly inhibited ACTH secretion in AtT-20 cells (Fig. 6I). Cell toxicity analyses confirmed that Lomitapide and Nicergoline were non-toxic to AtT-20 cells (Supplementary Fig. 6B-C), suggesting that their

inhibition of ACTH secretion was not due to cell death. Furthermore, immunohistochemical analysis and ELISA assays demonstrated that Lomitapide and Nicergoline reduced the protein levels of TPIT, POMC, and ACTH, leading to decreased ACTH secretion in vivo (Fig. 6J-K).

Taken together, Lomitapide and Nicergoline inhibit USP11 activity and exhibit anti-tumor effects in functioning ACTH PitNETs.

Discussion

This study demonstrates that USP11 promotes the deubiquitination of TPIT, resulting in enhanced ACTH secretion and an increased risk of Cushing's Disease in women. Virtual screening identified potential USP11 inhibitors, offering a promising therapeutic target and strategy for female patients with Cushing's Disease (Fig. 7).

Functioning ACTH PitNETs are complex neuroendocrine tumors that cause elevated ACTH levels, leading

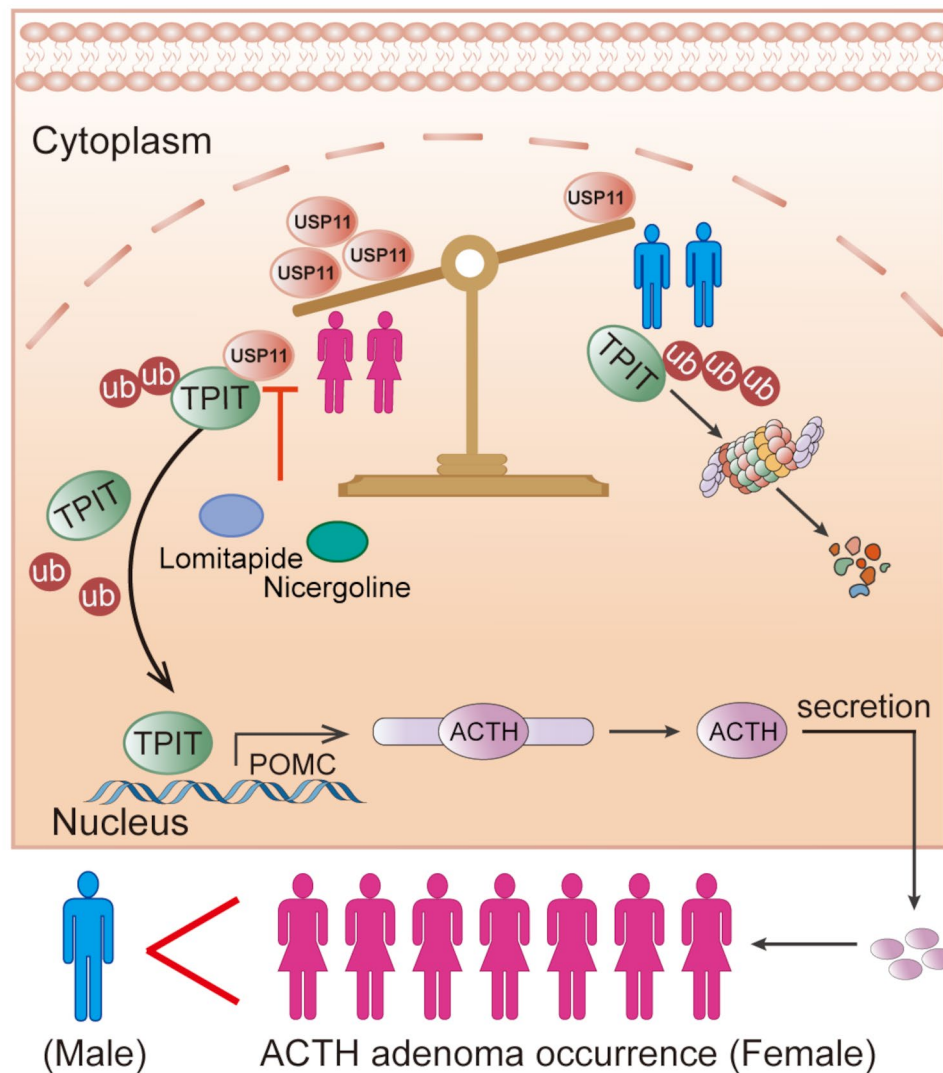


Fig. 7 USP11-mediated TPIT deubiquitination promotes the susceptibility of functioning ACTH adenoma in women

to Cushing's syndrome, a serious condition with high mortality if left untreated [2, 4]. These tumors are more prevalent in females, although the underlying reasons remain unclear, and they present significant treatment challenges. This study identifies USP11 as a susceptibility gene that may contribute to the higher incidence of functioning ACTH PitNETs in females. USP11 modulates the stability of the TPIT protein through deubiquitination, which in turn enhances the transcription of the POMC gene and the subsequent secretion of ACTH. This mechanism presents a potential therapeutic target for treating female patients with functioning ACTH PitNETs. However, the observed gender differences in tumor incidence may result from a complex interplay of factors, including genes on the sex chromosomes, genetic predispositions, hormonal influences, and immune system variations [21]. Regarding sex chromosomes-associated genes, some located on the X chromosome may escape the

inactivation process, leading to higher expression levels in females and a more prominent role in disease development [22, 23]. The mechanism by which the X-linked USP11 gene evades X chromosome inactivation warrants further investigation and could be crucial for understanding the gender disparities observed in functioning ACTH PitNETs. Furthermore, additional studies are needed to explore the role of other factors contributing to the differences between males and females in ACTH adenoma development.

The aberrant expression and activity of USP11 play a crucial role in the pathogenesis and progression of various diseases. USP11 regulates the stability and function of numerous disease-related proteins through its deubiquitination activity [24]. For instance, USP11 deubiquitinates EGFR, thereby stabilizing its protein levels and promoting partial epithelial-to-mesenchymal transition [19]. In colorectal cancer, USP11 promotes tumor growth

and metastasis via the ERK/MAPK pathway by stabilizing PPP1CA [18]. Estradiol stimulates USP11 expression, which in turn enhances the transcriptional activity of estrogen receptor alpha, correlating with poorer prognosis in breast cancer [15]. Furthermore, USP11 contributes to an increased risk of Alzheimer's disease in females by stabilizing tau protein, and inhibiting USP11 has been shown to slow disease progression [25, 26]. In this study, we identified two potential inhibitors targeting the functional domain of USP11, which effectively promote the ubiquitination and degradation of TPIT, thereby suppressing ACTH secretion. However, we did not observe evidence supporting the regulation of EGFR by USP11 in pituitary tumor cells and primary models. Additionally, estrogen and progesterone did not appear to influence the expression levels of USP11. These discrepancies may be attributed to variations in tumor types or differences between in vitro and in vivo models. Future research should further investigate the expression patterns, functional roles, and regulatory mechanisms of USP11 across various diseases and genders, which could inform the development of gender-specific cancer treatment strategies.

Treatment strategies for functioning ACTH PitNETs are continuously evolving. For instance, somatostatin analogs and pasireotide have been used to treat Cushing's disease [27]. Lomitapide, a pharmacological agent approved for the management of homozygous familial hypercholesterolemia, is associated with potential adverse effects such as diarrhea, indigestion, and a risk of hepatotoxicity [28]. In addition to its primary use in hypercholesterolemia, emerging evidence suggests that lomitapide may have therapeutic potential for various malignancies, including glioma and colorectal cancer [29, 30]. Research has shown that lomitapide can inhibit cancer cell proliferation and induce autophagic cell death by suppressing the mTOR signaling pathway [31]. Nicergoline, a pharmacological agent used to manage cognitive impairment, enhances cognitive function by modulating cerebral blood flow through its action on the central nervous system [32]. Although there are no reports suggesting that nicergoline can treat tumors, it has been shown to inhibit the PI3K/AKT signaling pathway [33]. Further research and clinical trials are needed to assess the potential efficacy of lomitapide and nicergoline in treating functioning ACTH PitNETs in females.

Conclusions

In summary, we found that USP11 expression is significantly elevated in female functioning ACTH PitNETs, with levels notably higher than those observed in male PitNETs and normal pituitary tissue. Experimental data suggest that USP11 promotes the deubiquitination of the key transcription factor TPIT in these PitNETs,

stabilizing its protein and thereby enhancing POMC transcription and ACTH secretion. Furthermore, virtual screening identified Lomitapide and Nicergoline as potential USP11 inhibitors, which were found to reduce POMC expression and ACTH secretion. Therefore, USP11 emerges as a potential therapeutic target, and inhibitors of its function could offer potential benefits for women with Cushing's disease.

Abbreviations

USP11	Ubiquitin Specific Peptidase 11
ACTH	Adrenocorticotrophic hormone
POMC	Proopiomelanocortin
PitNETs	Pituitary neuroendocrine tumors
AR	Androgen receptor
PAs	Pituitary adenomas
DMEM	Dulbecco's Modified Eagle Medium
IHC	Immunohistochemistry
qRT-PCR	Quantitative real-time PCR
MS	Mass spectrometry
MOI	Multiplicity of infection
Co-IP	Co-immunoprecipitation
CHX	Cycloheximide
GA	Genetic Algorithm
PSO	Particle Swarm Optimization
SEM	Standard error of the mean
ELISA	Enzyme-linked immunosorbent assay
GST	Glutathione S-transferase
TPIT	T-box transcription factor

Supplementary Information

The online version contains supplementary material available at <https://doi.org/10.1186/s40478-025-01938-9>.

Supplementary Material 1
Supplementary Material 1
Supplementary Material 3
Supplementary Material 4
Supplementary Material 5
Supplementary Material 6
Supplementary Material 7
Supplementary Material 8
Supplementary Material 9

Acknowledgements

We thank the investigators and research staff involved in this study.

Author contributions

Performed the experiments, analyzed the data, and co-wrote the manuscript: T.Z., Y.L. and F.L. Performed the data analysis: F.L. Performed CO-IP and immunoblotting experiments: K.G., R.T. and J.Y. Performed and analyzed the IHC experiments: L.X. Conceived the idea, designed and supervised the study, analyzed the data, and co-wrote the manuscript: Z.B.W. and Z.S.

Funding

This work was supported by the National Natural Science Foundation of China under Grant Number 82472640 (Z.B.W.), 82002627 (Y.L.), and 82172605 (L.X.). This work was also supported National Research Center for Translational Medicine under grant number NRCTM (SH) 2019-05 (Z.B.W.) and NRCTM (SH) 2023-15 (Z.B.W.) Key Research Project of Traditional Chinese Medicine of Zhejiang Province of China (GZY-ZJ-KJ-24087) of Z.S., Basic scientific research project of Wenzhou City of China (Y2023150) of Z.S.

Data availability

The raw sequence data reported in this paper have been deposited in the Genome Sequence Archive in National Genomics Data Center, China National Center for Bioinformation / Beijing Institute of Genomics, Chinese Academy of Sciences (GSA-Human: HRA005096) that are publicly accessible at <https://ngdc.cncb.ac.cn/gsa-human>.

Declarations

Ethics approval and consent to participate

Samples of pituitary adenomas (PAs) were obtained from patients undergoing surgical procedures at Ruijin Hospital between 2016 and 2023. The study received ethical approval from the Ethical Review Board of Ruijin Hospital, affiliated with Shanghai Jiao Tong University School of Medicine (China; 2019-39). The Ethical Review Board at Shanghai Jiao Tong University School of Medicine's Ruijin Hospital approved of the study's animal experimentation (China; RJ2023009).

Consent for publication

Not applicable.

Competing interests

The authors declare no competing interests.

Received: 29 November 2024 / Accepted: 25 January 2025

Published online: 05 February 2025

References

1. Tritos NA, Miller KK (2023) Diagnosis and management of Pituitary adenomas: a review, vol 329. *Jama*, pp 1386–1398
2. Melmed S, Kaiser UB, Lopes MB, Berthier J, Syro LV, Raverot G, Reincke M, Johannsson G, Beckers A, Flersieri M, Giustina A, Wass JAH, Ho KKY (2022) Clin Biology Pituit Adenoma *Endocr Rev* 43:1003–1037
3. Flersieri M, Varlamov EV, Hinojosa-Amaya JM, Langlois F, Melmed S (2023) An individualized approach to the management of cushing disease. *Nat Rev Endocrinol* 19:581–599
4. Hakami OA, Ahmed S, Karavitaki N (2021) Epidemiology and mortality of Cushing's syndrome. *Best Pract Res Clin Endocrinol Metab* 35:101521
5. Mindermann T, Wilson CB (1994) Age-related and gender-related occurrence of pituitary adenomas. *Clin Endocrinol (Oxf)* 41:359–364
6. Yaneva M, Kalinov K, Zachariva S (2013) Mortality in Cushing's syndrome: data from 386 patients from a single tertiary referral center. *Eur J Endocrinol* 169:621–627
7. Jimenez-Canizales CE, Rojas W, Alonso D, Romero I, Tabares S, Veronesi Zuluaga LA, Modica R, Colao A (2023) Clinical presentation and recurrence of pituitary neuroendocrine tumors: results from a single referral center in Colombia. *J Endocrinol Invest* 46:2275–2286
8. Zhang K, Shen M, Qiao N, Chen Z, He W, Ma Z, Shou X, Li S, Zhao Y, Pan L, Liu D, He M, Zhang Z, Li Y, Yao Z, Ye H, Wang Y (2020) Surgical outcomes and multidisciplinary management strategy of Cushing's disease: a single-center experience in China. *Neurosurg Focus* 48:E7
9. Yao H, Xie W, Dai Y, Liu Y, Gu W, Li J, Wu L, Xie J, Rui W, Ren B, Xue L, Cheng Y, Lin S, Li C, Tang H, Wang Y, Lou M, Zhang X, Hu R, Shang H, Huang J, Wu ZB (2022) TRIM65 determines the fate of a novel subtype of pituitary neuroendocrine tumors via ubiquitination and degradation of TPIT. *Neuro Oncol* 24:1286–1297
10. Ma ZY, Song ZJ, Chen JH, Wang YF, Li SQ, Zhou LF, Mao Y, Li YM, Hu RG, Zhang ZY, Ye HY, Shen M, Shou XF, Li ZQ, Peng H, Wang QZ, Zhou DZ, Qin XL, Ji J, Zheng J, Chen H, Wang Y, Geng DY, Tang WJ, Fu CW, Shi ZF, Zhang YC, Ye Z, He WQ, Zhang QL, Tang QS, Xie R, Shen JW, Wen ZJ, Zhou J, Wang T, Huang S, Qiu HJ, Qiao ND, Zhang Y, Pan L, Bao WM, Liu YC, Huang CX, Shi YY, Zhao Y (2015) Recurrent gain-of-function USP8 mutations in Cushing's disease. *Cell Res* 25:306–317
11. Chen J, Jian X, Deng S, Ma Z, Shou X, Shen Y, Zhang Q, Song Z, Li Z, Peng H, Peng C, Chen M, Luo C, Zhao D, Ye Z, Shen M, Zhang Y, Zhou J, Fahira A, Wang Y, Li S, Zhang Z, Ye H, Li Y, Shen J, Chen H, Tang F, Yao Z, Shi Z, Chen C, Xie L, Wang Y, Fu C, Mao Y, Zhou L, Gao D, Yan H, Zhao Y, Huang C, Shi Y (2018) Identification of recurrent USP48 and BRAF mutations in Cushing's disease. *Nat Commun* 9:3171
12. Dewson G, Eichhorn PJA, Komander D (2023) Deubiquitinases in cancer. *Nat Rev Cancer* 23:842–862
13. Dang F, Nie L, Wei W (2021) Ubiquitin signaling in cell cycle control and tumorigenesis. *Cell Death Differ* 28:427–438
14. Zhang X, Cheng L, Gao C, Chen J, Liao S, Zheng Y, Xu L, He J, Wang D, Fang Z, Zhang J, Yan M, Luan Y, Chen S, Chen L, Xia X, Deng C, Chen G, Li W, Liu Z, Zhou P (2023) Androgen Signaling contributes to sex differences in Cancer by inhibiting NF- κ B activation in T cells and suppressing Antitumor Immunity. *Cancer Res* 83:906–921
15. Dwane L, O'Connor AE, Das S, Moran B, Mulrane L, Pinto-Fernandez A, Ward E, Blümel AM, Cavanagh BL, Mooney B, Dirac AM, Jirstrom K, Kessler BM, T NC, Bernards R, Gallagher WM (2020) O'Connor, a functional genomic screen identifies the deubiquitinase USP11 as a Novel Transcriptional Regulator of ER α in breast Cancer. *Cancer Res* 80:5076–5088
16. Li X, Song N, Liu L, Liu X, Ding X, Song X, Yang S, Shan L, Zhou X, Su D, Wang Y, Zhang Q, Cao C, Ma S, Yu N, Yang F, Wang Y, Yao Z, Shang Y, Shi L (2017) USP9X regulates centrosome duplication and promotes breast carcinogenesis. *Nat Commun* 8:14866
17. Liu YT, Liu F, Cao L, Xue L, Gu WT, Zheng YZ, Tang H, Wang Y, Yao H, Zhang Y, Xie WQ, Ren BH, Xiao ZH, Nie YJ, Hu R, Wu ZB (2020) The KBTBD6/7-DRD2 axis regulates pituitary adenoma sensitivity to dopamine agonist treatment. *Acta Neuropathol* 140:377–396
18. Sun H, Ou B, Zhao S, Liu X, Song L, Liu X, Wang R, Peng Z (2019) USP11 promotes growth and metastasis of colorectal cancer via PPP1CA-mediated activation of ERK/MAPK signaling pathway. *EBioMedicine* 48:236–247
19. Shi Y, Tao M, Chen H, Ma X, Wang Y, Hu Y, Zhou X, Li J, Cui B, Qiu A, Zhuang S, Liu N (2023) Ubiquitin-specific protease 11 promotes partial epithelial-to-mesenchymal transition by deubiquitinating the epidermal growth factor receptor during kidney fibrosis. *Kidney Int* 103:544–564
20. Adasme MF, Linnemann KL, Bolz SN, Kaiser F, Salentin S, Haupt VJ, Schroeder M (2021) PLIP 2021: expanding the scope of the protein-ligand interaction profiler to DNA and RNA. *Nucleic Acids Res* 49:W530–w534
21. Shi Y, Ma J, Li S, Liu C, Liu Y, Chen J, Liu N, Liu S, Huang H (2024) Sex difference in human diseases: mechanistic insights and clinical implications. *Signal Transduct Target Ther* 9:238
22. Markaki Y, Gan Chong J, Wang Y, Jacobson EC, Luong C, Tan SYX, Jachowicz JW, Strehle M, Maestri D, Banerjee AK, Mistry BA, Dror I, Dossin F, Schöneberg J, Heard E, Guttman M, Chou T, Plath K (2021) Xist nucleates local protein gradients to propagate silencing across the X chromosome. *Cell* 184:6174–6192e6132
23. Tukiaainen T, Villani AC, Yen A, Rivas MA, Marshall JL, Satija R, Aguirre M, Gauthier L, Fleharty M, Kirby A, Cummings BB, Castel SE, Karczewski KJ, Aguet F, Byrnes A, Lappalainen T, Reguev A, Ardlie KG, Hacohen N, MacArthur DG (2017) Landscape of X chromosome inactivation across human tissues. *Nature* 550:244–248
24. Liao Y, Zhou D, Wang P, Yang M, Jiang N (2022) Ubiquitin specific peptidase 11 as a novel therapeutic target for cancer management. *Cell Death Discov* 8:292
25. Yan Y, Wang X, Chaput D, Shin MK, Koh Y, Gan L, Pieper AA, Woo JA, Kang DE (2022) X-linked ubiquitin-specific peptidase 11 increases tauopathy vulnerability in women. *Cell* 185:3913–3930e3919
26. Guo Y, Cai C, Zhang B, Tan B, Tang Q, Lei Z, Qi X, Chen J, Zheng X, Zi D, Li S, Tan J (2024) Targeting USP11 regulation by a novel lithium-organic coordination compound improves neuropathologies and cognitive functions in Alzheimer transgenic mice. *EMBO Mol Med*
27. Feelders RA, Newell-Price J, Pivonello R, Nieman LK, Hofland LJ, Lacroix A (2019) Advances in the medical treatment of Cushing's syndrome. *Lancet Diabetes Endocrinol* 7:300–312
28. Brahm AJ, Hegele RA (2016) Lomitapide for the treatment of hypertriglyceridemia. *Expert Opin Investig Drugs* 25:1457–1463
29. Song M, Tian J, Wang L, Dong S, Fu K, Chen S, Liu C (2024) Efficient delivery of Lomitapide using hybrid membrane-coated tetrahedral DNA nanostructures for Glioblastoma Therapy. *Adv Mater* 36:e2311760
30. Zuo Q, Liao L, Yao ZT, Liu YP, Wang DK, Li SJ, Yin XF, He QY, Xu WW (2021) Targeting PP2A with lomitapide suppresses colorectal tumorigenesis through the activation of AMPK/Beclin1-mediated autophagy. *Cancer Lett* 521:281–293
31. Lee B, Park SJ, Lee S, Lee J, Lee E, Yoo ES, Chung WS, Sohn JW, Oh BC, Kim S (2022) Lomitapide, a cholesterol-lowering drug, is an anticancer agent that induces autophagic cell death via inhibiting mTOR. *Cell Death Dis* 13:603

32. Fioravanti M, Flicker L (2001) Efficacy of nicergoline in dementia and other age associated forms of cognitive impairment, *Cochrane Database Syst Rev*, (2001) Cd003159
33. Zang G, Fang L, Chen L, Wang C (2018) Ameliorative effect of nicergoline on cognitive function through the PI3K/AKT signaling pathway in mouse models of Alzheimer's disease. *Mol Med Rep* 17:7293–7300

Publisher's note

Springer Nature remains neutral with regard to jurisdictional claims in published maps and institutional affiliations.